

# Tribological properties of silicon nitride ceramics modified by ion implantation

Naoki Nakamura<sup>a,\*</sup>, Kiyoshi Hirao<sup>b</sup>, Yukihiro Yamauchi<sup>b</sup>

<sup>a</sup>Synergy Ceramics Laboratory, Fine Ceramics Research Association, Shidami Human Science Park, Moriyama-ku, Nagoya, 463-8687 Japan

<sup>b</sup>Synergy Materials Research Center, National Institute of Advanced Industrial Science and Technology, Shidami Human Science Park, Moriyama-ku, Nagoya, 463-8687, Japan

## Abstract

Surface modification by ion implantation has been carried out in order to improve the tribological properties of gas-pressure sintered silicon nitride ceramics. B<sup>+</sup>, N<sup>+</sup>, Si<sup>+</sup> or Ti<sup>+</sup> ions were implanted into the silicon nitride ceramics with a fluence of  $2 \times 10^{17}$  ions/cm<sup>2</sup> at an energy of 200 keV. To evaluate the tribological properties of Si<sub>3</sub>N<sub>4</sub>, Block-on-Ring wear tests were conducted without lubricant, using the ion implanted Si<sub>3</sub>N<sub>4</sub> as block specimens and commercially supplied Si<sub>3</sub>N<sub>4</sub> as ring specimens. The specific wear rate of the ion-implanted Si<sub>3</sub>N<sub>4</sub> could be drastically reduced to a value of  $1.6 \times 10^{-9}$  mm<sup>3</sup>/N, accompanied by a decrease in the friction coefficient in the initial stage. According to surface analyses it was considered that the high wear resistance and low friction coefficient are attributed to the amorphization and the increase of surface hardness of the ion implanted layer.

© 2003 Elsevier Ltd. All rights reserved.

**Keywords:** Implantation; Si<sub>3</sub>N<sub>4</sub>; Surfaces; Wear parts; Wear resistance

## 1. Introduction

Because of their excellent mechanical properties, silicon nitride ceramics have created considerable interest in recent years for their potential application to automobile or power-generating industries.<sup>1–3</sup> Furthermore, silicon nitride ceramics are expected to be frictional materials<sup>4–8</sup> under conditions (e.g. high temperature, corrosion, vacuum, and magnetic fields) where metallic materials cannot be used, because of the superior properties of high strength, heat resistance, corrosion resistance, light weight, and insulation. However, it is necessary to improve the wear resistance of silicon nitride ceramics in order to allow their practical use. Since the mechanical and tribological properties of ceramics are very surface-sensitive, ion implantation is a possible tool to improve the tribological properties,<sup>9–13</sup> because it is possible to implant various kinds of atoms and control the surface structure at the atomic scale (see Fig. 1). The objective of this study is to improve the wear resistance of silicon nitride ceramics by means of ion implantation, whilst retaining the bulk properties

earlier described, and to clarify the effect of ion implantation on the tribological properties of silicon nitride ceramics.

## 2. Experimental

### 2.1. Fabrication of Si<sub>3</sub>N<sub>4</sub>

α-Si<sub>3</sub>N<sub>4</sub> powder (SN-E10, Ube Industries, Ltd., Japan) was mixed with 5 mass% Y<sub>2</sub>O<sub>3</sub> (Shin-Etsu Rare Earth, Ltd., Japan) and 2 mass% Al<sub>2</sub>O<sub>3</sub> (AKP-50, Sumitomo Chemical, Ltd., Japan) in ethanol for 2 h by planetary ball milling, followed by drying and pulverizing. The green bodies were then calcined at 800 °C for 2 h under N<sub>2</sub> gas at a flow rate of 1.5 l/min to remove organics. The calcined green bodies were cold isostatically pressed under 500 MPa after mold-pressing, and sintered at 1850 °C for 2 h in N<sub>2</sub> under a pressure of 0.9 MPa in a graphite crucible filled with a 70 mass% Si<sub>3</sub>N<sub>4</sub> and 30 mass% BN powder bed. The specimens could be densified to over 97% of theoretical density. The sintered Si<sub>3</sub>N<sub>4</sub> was machined into rectangular specimens of 3×4 mm with 1.55 mm thickness, for ion implantation followed by wear test.

\* Corresponding author.

E-mail address: [nakamura-naoki@aist.go.jp](mailto:nakamura-naoki@aist.go.jp) (N. Nakamura).

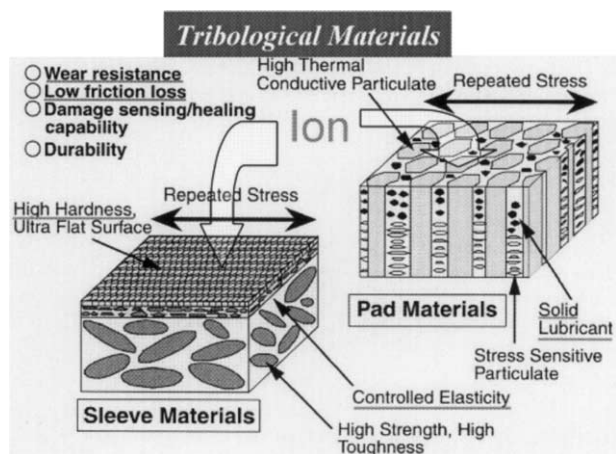


Fig. 1. Expectation of improvement of the wear resistance of  $\text{Si}_3\text{N}_4$  ceramics for ion implantation.

## 2.2. Ion implantation to $\text{Si}_3\text{N}_4$

Before implantation the specimens were cleaned with acetone in an ultrasonic bath. Boron, nitrogen, silicon or titanium ions were implanted into the mirror finished surfaces of the earlier-described silicon nitride ceramics with a fluence of  $2 \times 10^{17}$  ions/cm<sup>2</sup> at an energy of 200 keV. The ion implantation was carried out using a Freeman-type 400 keV ion implanter at the Ion Engineering Center Corporation, Osaka, Japan.  $\text{Si}_3\text{N}_4$  specimens were fixed to a 4-inch wafer and set in the vacuum chamber of the ion implanter. The ion source gas was introduced into the arc chamber and then ionized (generating plasma) by thermoelectrons from the filament.  $\text{BF}_3$ ,  $\text{N}_2$ ,  $\text{SiF}_4$  and  $\text{TiCl}_4$  were used as ion sources for  $\text{B}^+$ ,  $\text{N}^+$ ,  $\text{Si}^+$  and  $\text{Ti}^+$ , respectively. Generated ions were accelerated by the application of 30 V on the drawing electrode in front of

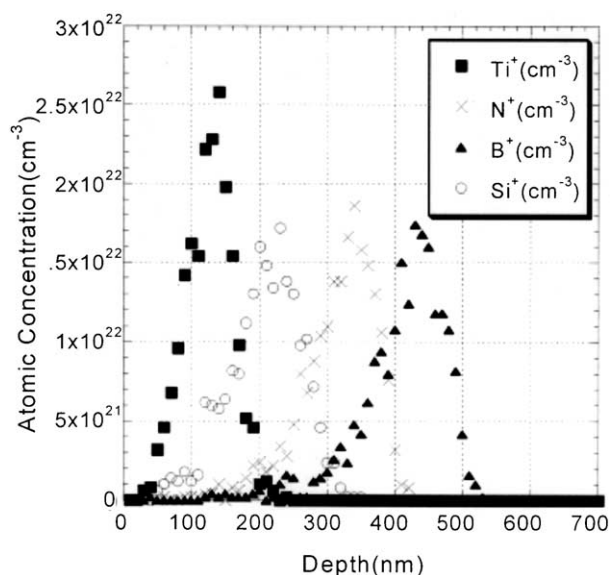


Fig. 2. Ion implantation profiles predicted by TRIM simulation.

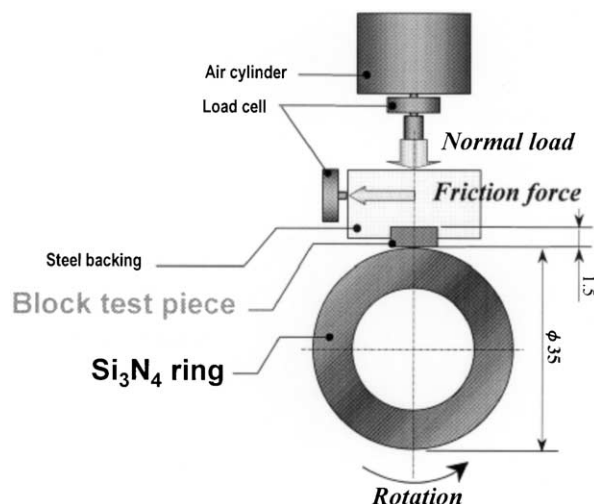


Fig. 3. Schematic view of block-on-ring wear tester.

the ion source, and 200 kV whole acceleration voltage on the acceleration electrode. Only the desired ions were extracted from various ions generated through the analysis electromagnet and slit. Ions were implanted uniformly throughout the whole implantation area in electrostatic scan mode by a beam scan. The expected implantation profiles, shown in Fig. 2, were estimated using the TRIM simulation. The surface-modified nano-structure of the ion implanted  $\text{Si}_3\text{N}_4$  was evaluated by Nanoindentation and Transmission Electron Microscopy.

## 2.3. Wear test

A block-on-ring type wear test machine (TRR-100D, Takachiho-Seiki Ltd., Japan) was used for friction and

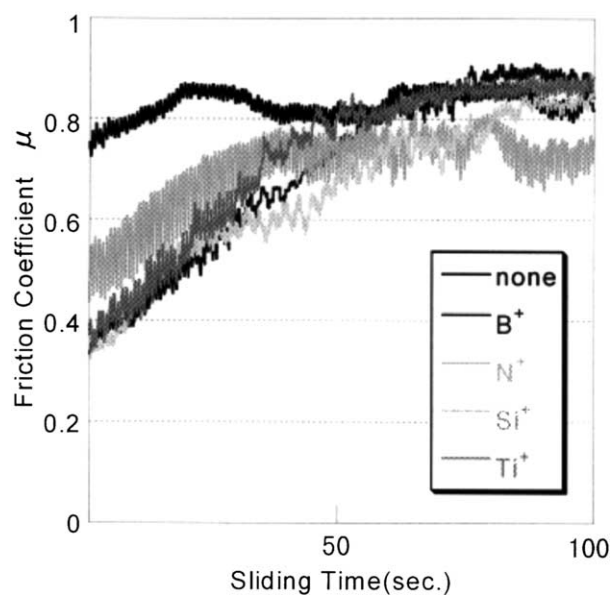


Fig. 4. Friction coefficient in the initial stage for  $\text{Si}_3\text{N}_4$  unimplanted and implanted with 200 keV ions.

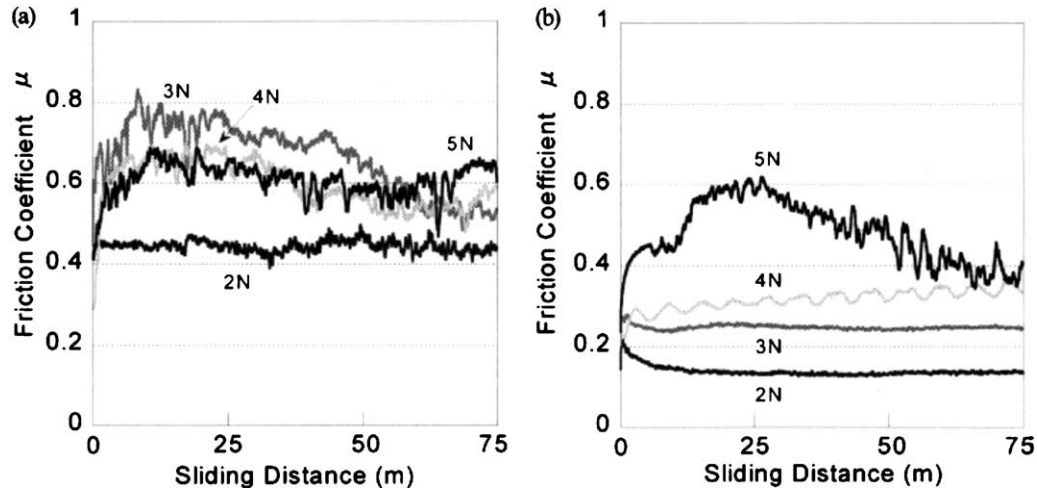


Fig. 5. Friction coefficient of  $\text{Si}_3\text{N}_4$  at a load of 2, 3, 4, 5 N: (a) unimplanted, (b)  $\text{Si}^+$ -implanted.

wear testing. The experimental setup used is illustrated in Fig. 3. Test samples described in Sections 2.1 and 2.2 were used for the block side and commercially supplied  $\text{Si}_3\text{N}_4$  (SN235P, Kyocera, Japan) was used for the ring test piece. To eliminate the contribution of lubricant, wear tests were conducted under dry conditions in air. Temperature and humidity were kept constant at  $25 \pm 3^\circ\text{C}$ ,  $25 \pm 2\%$  relative humidity, respectively. Sliding conditions were set at 0.15 m/s sliding speed, 2–5 N normal load, and 75 m sliding distance. The friction coefficient was recorded by monitoring the load and friction during the sliding test in real time using two sets of load cells. The wear volume was calculated by section analysis (analysis of nine lines) of the wear tracks, which were generated by the block-on-ring wear test, using a surface roughness tester (SV-624, Mitsutoyo, Japan). The specific wear rate ( $\text{mm}^2/\text{N}$ ) was obtained by dividing the wear volume ( $\text{mm}^3$ ) by the product of load (N)  $\times$  sliding distance (mm).

### 3. Results and discussion

#### 3.1. Influence of ion implantation on the tribological properties of $\text{Si}_3\text{N}_4$

Fig. 4 illustrates the variation of friction coefficient  $\mu$  in the initial stage. For the unimplanted specimen,  $\mu$  showed a large value of 0.8 over the whole sliding time range measured, even in the initial stage of the wear test. On the other hand, for the ion-implanted specimens,  $\mu$  showed a low value of 0.4 in the initial stage and a gradual increase with increase of sliding time. Fig. 5 shows variation of friction coefficients under different loads of 2, 3, 4 and 5 N. For the unimplanted  $\text{Si}_3\text{N}_4$ , there was little difference in the friction coefficient,  $\mu$ , under 3, 4, 5 N load. On the contrary, for the  $\text{Si}^+$ -implanted speci-

mens, there was an obvious dependence on normal load, that is to say, decreasing friction coefficient with lower normal load. Fig. 6 summarizes the specific wear rates for the  $\text{Si}_3\text{N}_4$  specimens in relationship to the ion species. Remarkable reduction of the specific wear rate was realized for each specimen of the ion-implanted  $\text{Si}_3\text{N}_4$ . For example, the specific wear rate of  $\text{Si}^+$ -implanted specimen was reduced to a value of  $1.64 \times 10^{-9} \text{ mm}^2/\text{N}$ , equal to a quarter of the unimplanted one. The specific wear rate of ion-implanted  $\text{Si}_3\text{N}_4$  showed ion species dependence, with the specific wear rate decreasing in the order of  $\text{B}^+ > \text{N}^+ > \text{Ti}^+ > \text{Si}^+$ . These ion species dependence is explained in terms of the implantation depth (see Fig. 2). The implanted layer prevented wear from progressing, and the shallower the implantation depth, the better is the wear resistance for  $\text{B}^+$ -,  $\text{N}^+$ -,

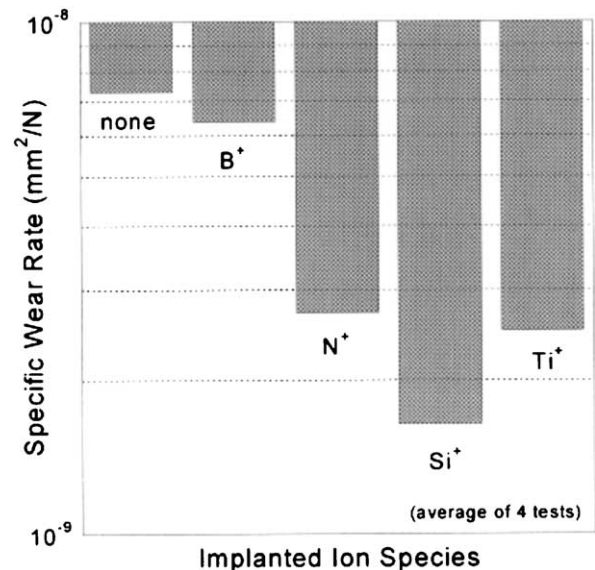


Fig. 6. Specific wear rates for unimplanted and implanted  $\text{Si}_3\text{N}_4$ .

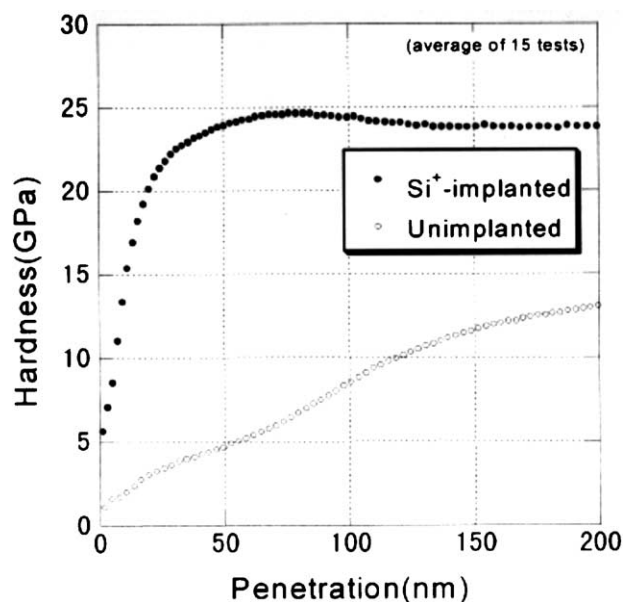


Fig. 7. Surface hardness of unimplanted and implanted  $\text{Si}_3\text{N}_4$  evaluated by Nanoindentation.

$\text{Si}^+$ -implanted specimens because most of the implanted ions are located at the near surface region. As for the  $\text{Ti}^+$ -implanted specimen, the peak value of implanted atomic concentration is higher than the other ion species and the atomic radius is also largest (Ti: 1.45 Å, B: 0.9 Å, N: 0.75 Å, Si: 1.15 Å), which may have broken the Si–N bond, leading to less wear resistance compared with  $\text{Si}^+$  case.

### 3.2. Structural investigation of ion-implanted $\text{Si}_3\text{N}_4$

In order to clarify the effect of ion implantation on the tribological properties of  $\text{Si}_3\text{N}_4$ , Nanoindentation method was used for measuring surface hardness and cross-sectional TEM was used for observing the microstructure of surface-modified  $\text{Si}_3\text{N}_4$ . The nanoindentation was carried out using a nanoindenter (Nano Indenter XP, MTS Systems Corporation, USA). The surface hardness is plotted against the penetration depth in Fig. 7. It can be clearly seen that the  $\text{Si}^+$ -implanted surface is harder than the unimplanted surface. For the unimplanted  $\text{Si}_3\text{N}_4$ , the hardness increases gradually up to a penetration depth of 200 nm. In contrast, for the  $\text{Si}^+$ -implanted  $\text{Si}_3\text{N}_4$ , the hardness shows a sharp rise just near the surface, followed by saturation state at around 50 nm. The hardness of  $\text{Si}^+$ -implanted  $\text{Si}_3\text{N}_4$  increases by 80% to 23.5 GPa compared with the unimplanted  $\text{Si}_3\text{N}_4$  at 200 nm. In general, the hardness of a material increases with decreasing the interatomic distance, so the hardness increase is considered to be due to the densification caused by ion implantation, resulting in the low friction and high wear resistance.

A cross-sectional TEM (H-9000UHR III, Hitachi, Japan) micrograph of  $\text{Si}^+$ -implanted  $\text{Si}_3\text{N}_4$  is shown in Fig. 8. Directly at the surface a 350 nm wide gray band is visible in the  $\text{Si}^+$ -implanted  $\text{Si}_3\text{N}_4$ , while no such band was observed in the unimplanted  $\text{Si}_3\text{N}_4$ . The electron diffraction patterns in Fig. 8(b) are from the locations indicated by the arrows. The observed broad

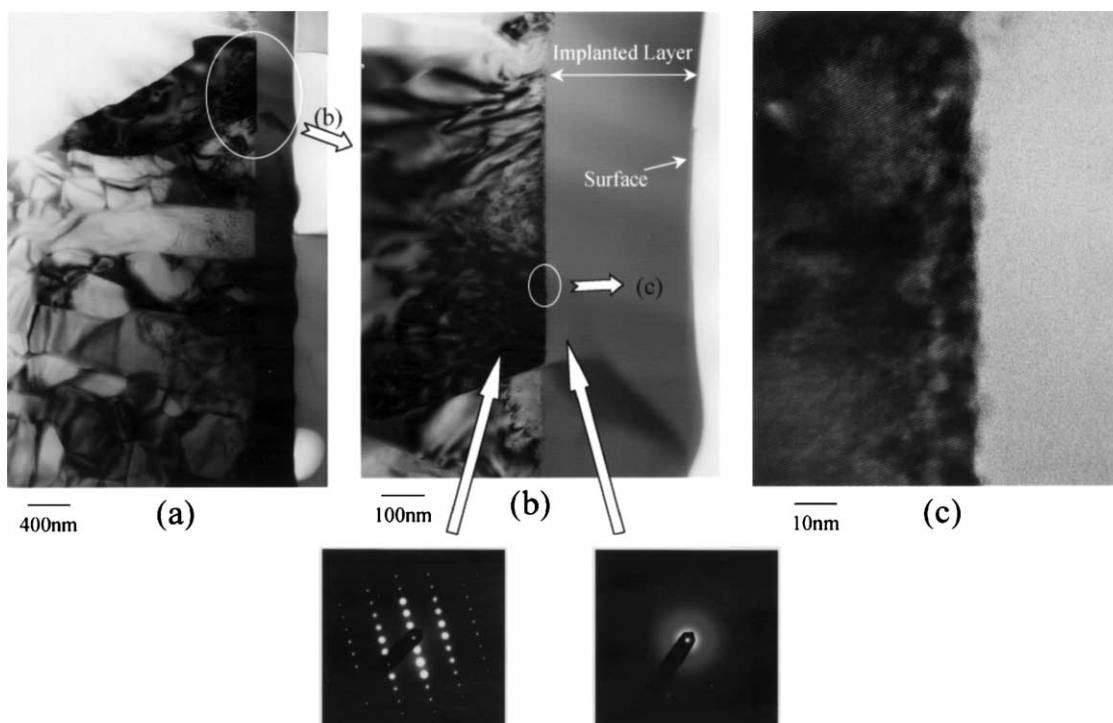


Fig. 8. Cross-sectional TEM micrographs of the  $\text{Si}^+$  implanted  $\text{Si}_3\text{N}_4$  with electron diffraction patterns.



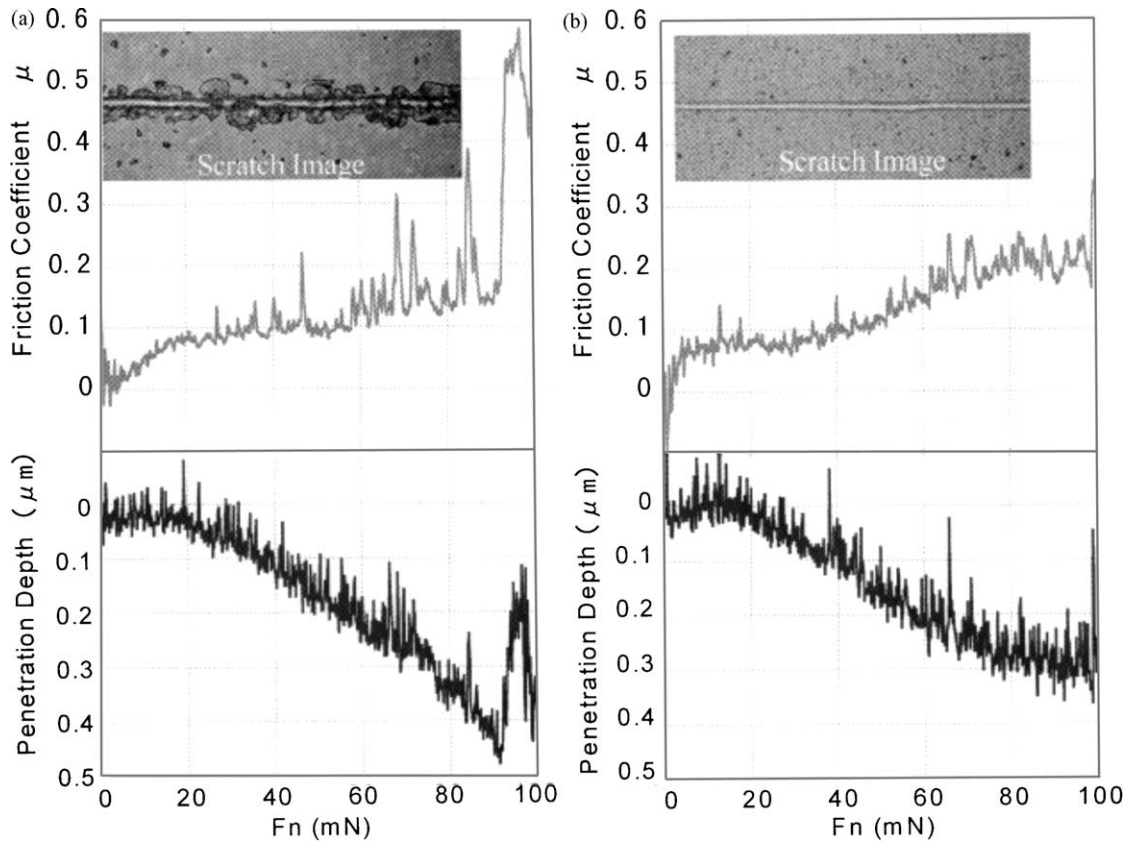


Fig. 9. Results of the scratch tests for unimplanted and  $\text{Si}^+$ -implanted  $\text{Si}_3\text{N}_4$ ; (a) unimplanted, (b)  $\text{Si}^+$ -implanted.

fringes indicate that the gray region is amorphous. The depth of the amorphized region is in fairly good agreement with the ion-implanted region predicted by TRIM (see Fig. 2). Thus, the tribological properties of silicon nitride ceramics are considered to be strongly affected by the surface amorphization. Based on the earlier results, it is considered that the high wear resistance and low friction of the ion implanted  $\text{Si}_3\text{N}_4$  are attributed to the increase of surface hardness, the surface shear stress relaxation and the prevention of grain boundary related crack initiation due to the surface amorphization.

In order to prove this wear mechanism, nano-scratch test was conducted using a scratch tester (Nano-Scratch Tester, CSM Instruments, Switzerland). A spherical diamond indenter of radius  $2\text{ }\mu\text{m}$  was used with a loading rate of  $140\text{ mN/min}$ . The results presented in Fig. 9 show progressive load measurements over the range  $0\text{--}100\text{ mN}$  on the surfaces of the unimplanted and  $\text{Si}^+$ -implanted  $\text{Si}_3\text{N}_4$ . For the unimplanted specimen, friction coefficient fluctuated on a large scale, followed by a sharp rise to 0.5 at  $90\text{ mN}$ , which is identified as chipping after the optical microscope observation. On the other hand, the friction coefficient of the  $\text{Si}^+$ -implanted specimen showed less fluctuations and lower values over the whole range of normal force, without chipping as is shown in the optical micrograph. Thus, the nano-scratch results are consistent with the wear mechanism speculated earlier.

#### 4. Conclusion

Surface modification by ion implantation has been carried out in order to improve the tribological properties of  $\text{Si}_3\text{N}_4$ .  $\text{B}^+$ ,  $\text{N}^+$ ,  $\text{Si}^+$  or  $\text{Ti}^+$  ions were implanted into the mirror-finished surface of silicon nitride ceramics with a fluence of  $2 \times 10^{17}\text{ ions/cm}^2$  at an energy of  $200\text{ keV}$ . The wear behavior of the ion-implanted  $\text{Si}_3\text{N}_4$  was evaluated using a block-on-ring wear tester, and related to the effect of surface modification by ion implantation. Both the friction coefficient and the specific wear rate were reduced by ion implantation. The specific wear rate of  $\text{Si}^+$ -implanted specimen, which showed the greatest improvement, was reduced to a value of  $1.64 \times 10^{-9}\text{ mm}^2/\text{N}$ , equal to a quarter of the unimplanted one. According to surface analyses, the high wear resistance and low friction coefficient were attributed to the surface amorphization and the increase of surface hardness of the ion implanted layer.

#### Acknowledgements

This work has been supported by METI, Japan, as part of the Synergy Ceramics Project. Part of the work has been supported by NEDO. The authors are members of the Joint Research Consortium of Synergy Ceramics.

## References

1. Woetting, G., Leimer, G., Linder, H. A. and Gugel, E., Silicon nitride materials and components for industrial application. *Industrial Ceramics*, 1995, **15**(3), 191–196.
2. Hirao, K., Brito, M. E., Toriyama, M., Kanzaki, S. and Teshima, H., Effect of seed alignment on microstructures and mechanical properties of silicon nitride. In *Proceedings of Sintering Science and Technology*, ed. R. M. German, G. L. Messing and R. G. Cornwall. the Pennsylvania State University, PA., USA, 2000, pp. 343–348.
3. Teshima, H., Hirao, K., Toriyama, M. and Kanzaki, S., Fabrication and mechanical properties of silicon nitride ceramics with unidirectionally oriented rodlike grains. *J. Ceram. Soc. Japan*, 1999, **107**(12), 1216–1220 [in Japanese].
4. Muratov, V. A., Luangvaranunt, T. and Fischer, T. E., The tribochemistry of silicon nitride: effects of friction, temperature and sliding velocity. *Tribology International*, 1998, **31**(10), 601–611.
5. Xingzhong, Z., Jiajun, L., Baoliang, Z., Hezhou, M. and Zhenbi, L., Wear behavior of  $\text{Si}_3\text{N}_4$  ceramic cutting tool material against stainless steel in dry and water-lubricated conditions. *Ceramics International*, 1999, **25**, 309–315.
6. Zutshi, A., Haber, R. A., Niesz, D. E., Adams, J. W., Wachtman, J. B., Ferber, M. K. and Hsu, S. M., Processing, microstructure, and wear behavior of silicon nitride hot-pressed with alumina and yttria. *J. Am. Ceram. Soc.*, 1994, **77**(4), 883–890.
7. Liang, Y. N., Lee, S. W. and Park, D. S., Effects of whisker distribution and sintering temperature on friction and wear of  $\text{Si}_3\text{N}_4$ -whisker-reinforced  $\text{Si}_3\text{N}_4$ -composites. *Wear*, 1999, **225–229**, 1327–1337.
8. Nakamura, M., Hirao, K., Yamauchi, Y. and Kanzaki, S., Tribological properties of unidirectionally aligned silicon nitride. *J. Am. Ceram. Soc.*, 2001, **84**(11), 2579–2584.
9. Brenscheidt, F., Wieser, E., Matz, W., Mücklich, A. and Möller, W., Tribological properties of chromium implanted silicon nitride ceramics correlated with microstructure. *Applied Physics A*, 1997, **65**, 281–286.
10. Brenscheidt, F., Oswald, S., Mücklich, A., Wieser, E. and Möller, W., Wear mechanisms in titanium implanted silicon nitride ceramics. *Nuclear Instruments and Methods in Physics Research B*, 1997, **129**, 483–486.
11. Tanaka, T., Nakayama, H., Sekiya, H., Sekine, K. and Umehara, K., Friction and wear properties of  $\text{N}^+$  ion-implanted silicon nitride. *J. Soc. Mat. Sci., Japan*, 1997, **46**(11), 1293–1299 [in Japanese].
12. Morrison, J. A., Thakker, A. B. and Armini, A. J., Ion implantation of silicon nitride for rolling element bearing applications. *Ceram. Eng. Sci. Proc.*, 1988, **9**(9–10), 1265–1275.
13. Williams, J. M. and Miner, J. R., Ion implantation of silicon nitride ball bearings. *Nuclear Instruments and Methods in Physics Research B*, 1997, **127/128**, 981–986.